Published by
NIGERIAN SOCIETY OF PHYSICAL SCIENCES
Available online @ https://journal.nsps.org.ng/index.php/jnsps

J. Nig. Soc. Phys. Sci. 5 (2023) 1222

Journal of the Nigerian Society of Physical Sciences

Tuning the optical properties and some surface structure of Cd-O thin film electrodeposited by two-electrode: An effect of Cobalt incorporation

Rafiu A. Busari[a,b,*], Ezekiel Omotoso[b], Lukman O. Animasahun[b,c], Saheed A. Adewinbi[d], Emmanuel O. Adewumi[b], Comfort T. Famoroti[b], Bidini A. Taleatu[b], Adeniyi Y. Fasasi[e]

[a]*Department of Physics, Nigerian Army University, Biu, Nigeria*
[b]*Department of Physics and Engineering Physics, Obafemi Awolowo University, Ile-Ife 220005, Nigeria*
[c]*Department of Physics, Electronics and Earth Sciences, Fountain University, Osogbo, Nigeria*
[d]*Department of Physics, Osun State University, Osogbo 210001, Nigeria*
[e]*Centre for Energy Research and Development, Obafemi Awolowo University, Ile-Ife 220005, Nigeria*

Abstract

The tuning of optical and dielectric parameters, structural and microstructural properties of CdO synthesized via a solution growth two-electrode cell arrangement under ambient environment, with the incorporation of Co ion into its matrix was investigated. The energy band gaps of the films was estimated in the range of 1.69 eV ≤ Eg ≤ 1.96 eV. The extinction coefficient, k for all the samples decreases as the incident photon energy increases. The films exhibit considerably high optical conduction across the photon energy with estimated power of 10^{13} $(\Omega m)^{-1}$. The elemental composition of the samples was determined using the energy dispersive x-ray spectrometry technique. The micrograph images from scanning electron microscopy technique shown that the films are polycrystalline and well-adhered to the substrates with their crystal grains evenly dispersed across the substrates' surface. The x-ray diffraction analysis confirmed that the deposited films are of polycrystalline in nature. The films show preference for orientation along the (111) plane.

DOI:10.46481/jnsps.2023.1222

Keywords: Polycrystalline; solar cell; electrochemical deposition; direct band gap; transparent conducting oxide

Article History :
Received: 23 November 2022
Received in revised form: 31 January 2023
Accepted for publication: 14 February 2023
Published: 02 May 2023

Communicated by: Edward Anand Emile (PhD)

1. Introduction

In the fields of microelectronics, optical coatings, integrated optics, superconductors, and other technologies, thin film technologies have been crucial [1, 2]. The use of II-VI group n-type semiconducting materials as well as the synthesis of different compositions of these materials have grown tremendously in recent years. This is due to their scientific importance and a wide range of potential uses in optoelectronic devices and applications. Many scientist and researchers are interested in the binary, ternary as well as the quaternary forms of these materials because of the possibility of controlling, tuning, and modifying their physical, optical, and electrical properties [3]. Deposited

*Corresponding author tel. no: +2348064244378
Email address: rafiu.busari@naub.edu.ng, rafiuwaleb@gmail.com (Rafiu A. Busari)

oxide thin films such as those of Sn, Cd, Zn, Ti, and so on and the incorporation of appropriate dopant impurities, have formed a range of useful synthetic transparent conductors applicable in solar cells, optoelectronic, and energy storage devices [1, 2, 4].

Cadmium oxide (CdO), a reddish powder is a transparent conducting oxide. It is a semiconducting material of the II-VI group that is n-type, having a direct energy band gap of around 2.0 eV. Each atom in the cubic structure of this substance is surrounded by six other atoms with the opposite electrical charge. The material exhibits a cubic crystal structure [4,5]. CdO nanostructures, even without doping have a low ohmic resistance, a considerably high optical transmittance in the solar spectrum's visible range, and a moderate refractive index. These features have potential uses in optoelectronic field such as transparent electrodes, photovoltaic cells, photodiodes, phototransistors as well as gas sensors [4]. The crucial factors in these applications includes specific surface area, particle size, and porosity. Up to recent time, different CdO nanostructures, including nanowires, nanoneedles, nanobelts, nanoclusters, nanorods, and nanoparticles have so far been synthesized via different chemical and physical techniques. These include; vapour phase transport, spray pyrolysis, sputtering, template-assisted, MOCVD, solvothermal and so on. By calcining hydroxyl and carbonate-containing cadmium compound precursor at 500 ^{o}C in air for two hours, Guo *et al.* were able to prepare porous CdO nanowires that were around 100 μm long and 120 nm in diameter [6]. CdO nanotubes was fabricated by Lu *et al.* using thermal evaporation of Cd powder under moderate pressure and temperature of 500 ^{o}C [7]. The use of intricate precursor materials, drawn-out experimental procedures, expensive and sophisticated equipment and atmosphere controlled heating regimes have all compounded the aforementioned methods.

In the present work, we investigated the effects of Co ion dopant on the optical, structural and microstructural performance of two-electrode electrodeposited CdO thin film. This synthesis method is a simple, cost effective, scalable and easy to operate technique. Its ability to produce materials for a variety of uses, including optical mirrors, photosensitive devices, integrated circuits, colour television screens, magnetic disks, and more, makes it distinctive [2,8,9].

2. Experimental procedure

2.1. Materials

In the experiment, we employed the use of cadmium chloride ($CdCl_2$; 98%), sodium hydroxide (NaOH; 99.99%), cobalt chloride ($CoCl_2$; 99.99%), glass pieces coated with indium-tin oxide (ITO) as substrates with surface resistivity of 15/ sq.meter and ($20 \times 15 \times 0.7$) mm dimensions in the deposition process. Distilled water was used as the solvent. All the reagents used in this experiment were analytical grade (Sigma-Aldrich). The ITO substrates were cleaned as reported in our previous work [8]. Following a thorough cleaning with a cotton-bud and soap solution, the substrates were rinsed under running water and ultrasonically treated with distilled water, acetone, and methanol for 10 minutes each at a temperature of 40 ^{o}C. After cleaning, the substrates were dried at a moderate temperature in an open furnace. All of these actions were taken to clean the substrates' surface of any potential impurities.

2.2. Samples preparation

Deposition of CdO and Co-doped CdO thin films were done by a two-electrode set-up arrangement. The cell involves a glassy-carbon piece and a conductive substrate (ITO) as counter and working electrodes, respectively. For the deposition of undoped CdO (Tag: X1), an electrolyte was made from the mixture of 20 mL of 0.2 M; $CdCl_2$ and 20 mL of 0.1 M; NaOH and the resultant was fed to the cell. The electrodes were then fastened to the holder already connected to D. C. source and a digital multi-meter with sensitive current and voltage modes selected to achieve stability in power supply according to the reports in [2,8]. The experiment was conducted at a cathodic potential of 1.9 V. The sample growth was monitored through the multi-meter as the current degrades. Optimum growth of the sample X1 was then achieved after 25 min of deposition at ambient temperature. For the growth of Co-doped CdO samples, electrolyte formed for sample X1 was modified by adding 10 ml of 0.05 M of $CoCl_2$ for the deposition of sample X2 and 10 ml of 0.1 M of $CoCl_2$ for the position of sample X3, respectively. After the optimum growth is obtained, all the three samples were taken out of the bath, distillated, and then dried for 5 minutes at 120 ^{o}C in an open furnace to eliminate any remaining water content and other potential adsorbed surface contaminants [8]. All the deposited films were annealed in air with constant temperature of 350 ^{o}C for 1 hour. This process was done to make sure the films were as crystalline as possible and to position the particles in the right equilibrium sites.

2.3. Samples characterization

An X-ray diffraction via the XPERTPRO diffractometery, PANalytical BV with wavelength of 1.5406 Å and Cu$K\alpha$ as radiation source was used to analyze the materials' structural composition. Surface micrograph of the samples was obtained from scanning electron microscopy (SEM) (ZEISS ultra-plus 55). The films' elemental composition was investigated using energy dispersive X-ray spectrometry technique. Samples' optical characteristics were analysed on a double beam spectrophotometer (Shimadzu UV-1800).

3. Results and discussion

3.1. Chemical composition

Energy dispersive X-ray spectroscopy was used to analyze the pure and Co-doped samples' chemical composition, as shown in the Fig. 1. Figure 1(a) shows the spectrum of the undoped sample with peaks of cadmium and oxygen, while Figure 1 (b) shows the spectrum of the doped sample with peaks of cadmium, cobalt and oxygen. The obtained results supported the thin film deposition of CdO and Co-doped CdO.

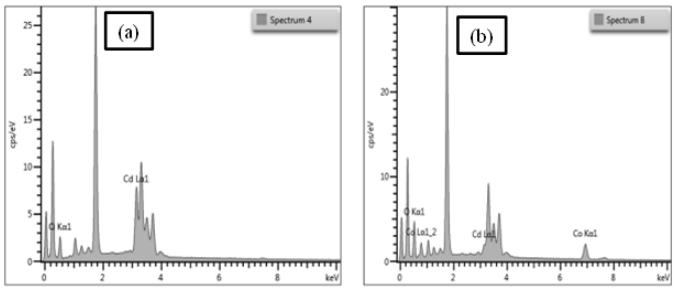

Figure 1: EDX spectrum of (a) CdO thin film; (b) Co-CdO thin film

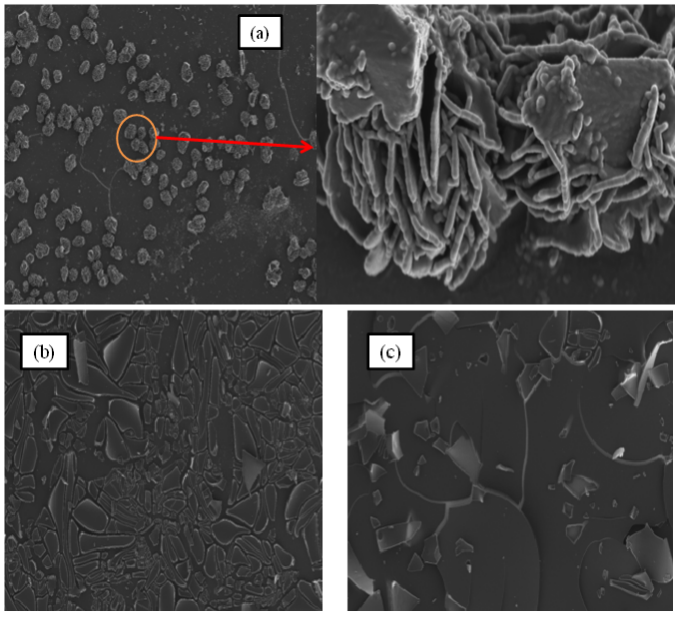

Figure 2: SEM images of (a) pure CdO, (b) Co-CdO @ 0.05 M and (c) Co-CdO @ 0.1 M

3.2. Morphological studies

Morphological investigation plays important roles in appraising the films' nature and their surface properties. The micrograph images of the electrodeposited CdO and Co-CdO films analyzed by SEM are shown in the Fig. 2. It is seen from the micrograph images of the deposited samples, a smooth and homogeneous surface morphology. Fig. 2 (a) revealed the distribution of sphere-like with fused rice-like particles across the substrate's surface. It is seen from the images that the surface characteristic of the CdO film particles changes as of Co ion concentration rises. The incorporation of the Co-impurity is also seen to have introduced crack and void into the host's structure. These obvious varying characteristics are due to the enormous variation ~ 32% in ionic radius between cadmium with 0.095 nm and cobalt with 0.065 nm. Co's atomic radii is 125 pm, while Cd's is 151 pm, respectively. The development of morphologies may be concerned with various atomic radii and electronegativities of the dopant ions, which have an impact on the thermodynamically stable growth process of the free surfaces of CdO thin film crystal faces [10].

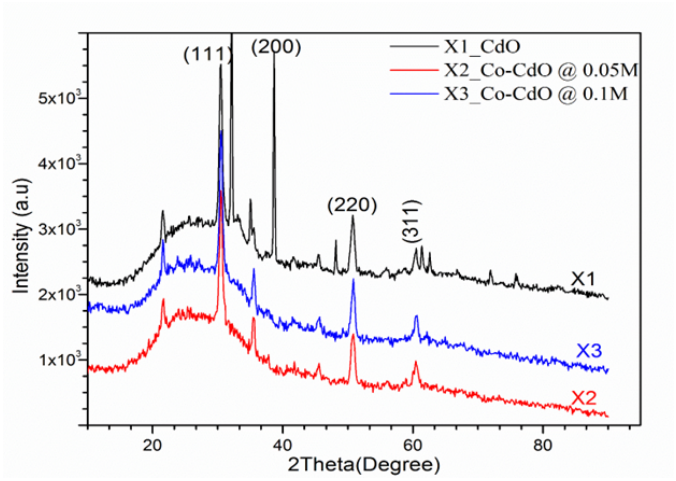

Figure 3: X-ray diffraction pattern of the CdO and Co-doped CdO thin films

3.3. Structural analysis

To learn more about the CdO film's crystallinity and crystallite size, an X-ray diffraction technique was conducted. The X-ray diffraction patterns for pure and CdO doped Co ion thin films are shown in Fig. 3. The patterns' many peaks suggest that they are polycrystalline cubic (Fm-3m) CdO thin film structure with lattice parameter of ~ 0.474 nm, which is near the value of 0.46948 nm for CdO [11]. Using the ASTM standard, the identified peaks in the patterns can be indexed to the (111), (220) and (311) planes [12]. In a polycrystalline material, the crystallites typically involve differential crystallographic orientation among their neighbours. In relation to some chosen frame of reference, this preference orientation may be dispersed randomly. In the present work, the films exhibit a preferential orientation along the (111) diffraction plane. The texture coefficient $Tc_{(hkl)}$ measured from the samples was used to appraise the possibility of the preference orientation. The $Tc_{(hkl)}$ has been examined from the X-ray diffraction data using the expression below [12,13]:

$$Tc_{(hkl)} = \frac{I_{(hkl)}/\ I_{o(hkl)}}{N_r^{-1} \sum_{N_r} I_{(hkl)}/I_{o(hkl)}}, \tag{1}$$

where $I_{(hkl)}$ is intensity of the *(hkl)* plane, $I_{o(hkl)}$ is the reference corresponding powder (ASTM standard), while N_r is referred to the reflection number. From the definition, it shows that the deviation of texture coefficient from unity signifies the growth's preferred orientation.

The Debye-Scherer's equation was used to evaluate the crystallite size (D) of the samples [14].

$$D = \frac{0.94\ \lambda}{\beta cos\theta}, \tag{2}$$

where λ is the wavelength of the CuK radiation, β is the diffraction peak's FWHM, and while θ is the Bragg's diffraction angle. The estimated crystallite size and some other structural data are presented in Table 1. It shows that the D values of the films were dependent on the dopant molar concentration.

The micro-strain and dislocation density of the deposited films were also calculated from the following relations [14]:

$$\text{Microstrain}\,(\varepsilon) = \frac{\beta cos\theta}{4}, \tag{3}$$

$$\delta = \frac{1}{D^2}. \tag{4}$$

3.4. Optical characterisation

3.4.1. Optical absorption and transmission studies

Optical absorption study plays important roles in the understanding of various semiconductor and non-metallic materials' structural band nature [15,16]. UV-visible spectrum has been utilized to determine the absorption coefficient (α), energy band gap (E_g), extinction coefficient (k), refractive index (n), optical conductivity (σ_{opt}), and other parameters for all the deposited samples. Fig. 4(a) represents the absorbance spectra of the pure and Co-doped CdO thin films. It is evident from the spectra that the samples absorption strength is generally dependent on the dopant concentration. It is seen that sample X3 has the highest absorption power across the wavelength region. Inset is the variation of the percentage optical transmission with wavelength, within the wavelength range of 200 – 900 nm. It is observed that as the dopant concentration increases, the samples' percentage transmission decreases across the wavelength region from around 93 to 57 %. Similar results have also been reported in [10,13]. It is also worthy to point out that the films transmission across the wavelength region strongly dependent on the film's thickness.

The absorption coefficient (α) was estimated via the Beer-Lambert relation in equations (5 and 6) using the absorbance (A) and transmittance (T) data [16,17].

$$I = I_O e^{-\propto t}, \tag{5}$$

$$\propto = \frac{\ln(I_o/I)}{t} = -\left(\frac{lnT}{t}\right) = \frac{2.303A}{t}, \tag{6}$$

where I and I_o are instantaneous and initial intensities of the photon and while t is the film's thickness. The films' thickness was determined by the gravimetric weight difference technique using the relation below [18]:

$$t = \frac{m}{Ad}, \tag{7}$$

where m is mass of the prepared sample, A is area of the laminated sample on the substrate and d sample's density. The estimated values of m, A, d and t are presented in Table 1.

The plot of absorption coefficient (α) as a function of incident wavelength within the range 200 – 900 nm is shown in the Fig. 4(b). The value of α is considerably high for all the samples up till around 300 nm and at higher wavelength as seen from the figure, the value of α is observed to be nearly invariant for all the samples. This behaviour may be attributed to the lattice deformation or internal electric fields as owing to strain [16].

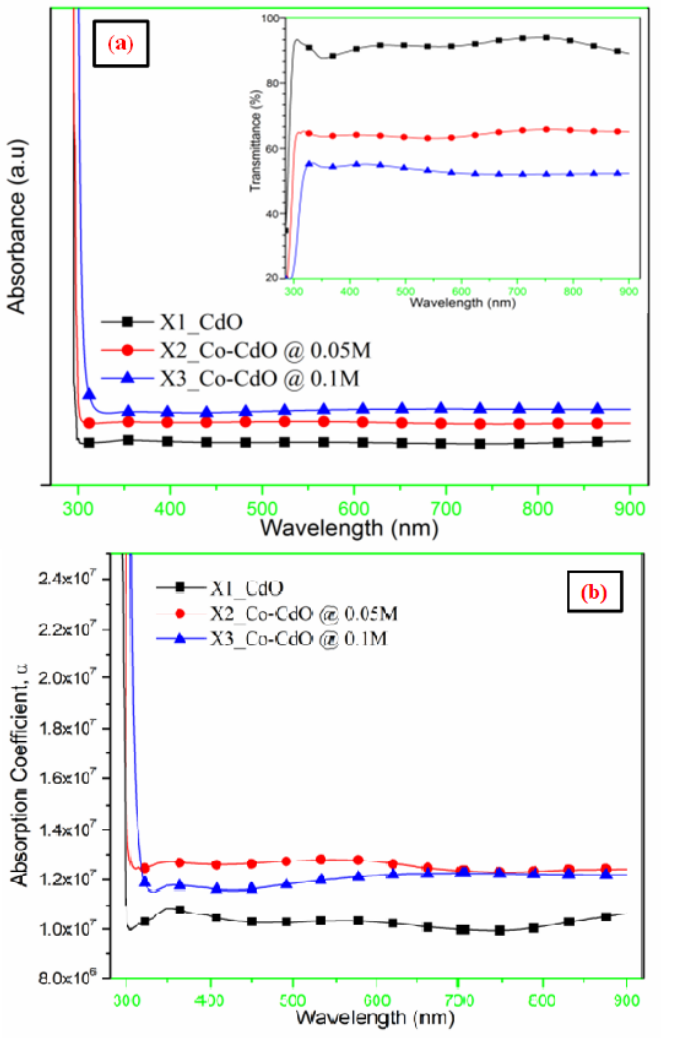

Figure 4: (a)UV-Vis absorbance spectra of the thin films (Inset: variation of optical transmission with wavelength). (b) Optical absorption coefficient against incident wavelength of the deposited films

3.4.2. Energy band gap

The samples energy band gap was determined from the relation [8,19]:

$$\propto h = A(h - E_g)^n, \tag{8}$$

where A, v, h and n are the empirical constant, frequency of the incident light, Planck's constant and power factor, respectively. Thin film power factor depends on transition nature and which may have values from $\frac{1}{2}$, $\frac{3}{2}$, 2 or 3 representing direct allowed, direct forbidden, indirect allowed or indirect forbidden. Value of n for the present work is $\frac{3}{2}$ for determining the energy band gaps from the optical absorption data. By estimating the band gaps, we extrapolate the linear portion of the plot of $(\alpha h\nu)^2$ against $h\nu$ at when $(\alpha h\nu)^2 = 0$. This gives the value of energy band gap as shown in the Fig. 5. The obtained direct allowed band gaps for the samples X1, X2 and X3 are 1.96, 1.69 and 1.71 eV, respectively. The obtained energy band gaps for pure and doped CdO films are in good agreement with the literature [10, 13, 20]. It is observed that the film's energy band

Table 1: Some estimated parameters from XRD pattern and thickness of the deposited samples

Tag	a (Å)	D (nm)	ε($\times 10^{-4}$)	δ($\times 10^{-4}$)(lines/nm)	m (mg)	A (cm^2)	d (g/ml)	Thickness, t(nm)
X1	4.83	38.74	8.27	6.66	0.15	1.5	8.15	120
X2	4.74	41.82	7.51	5.72	0.26	1.5	8.53	200
X3	4.65	43.68	7.08	5.24	0.31	1.5	8.53	240

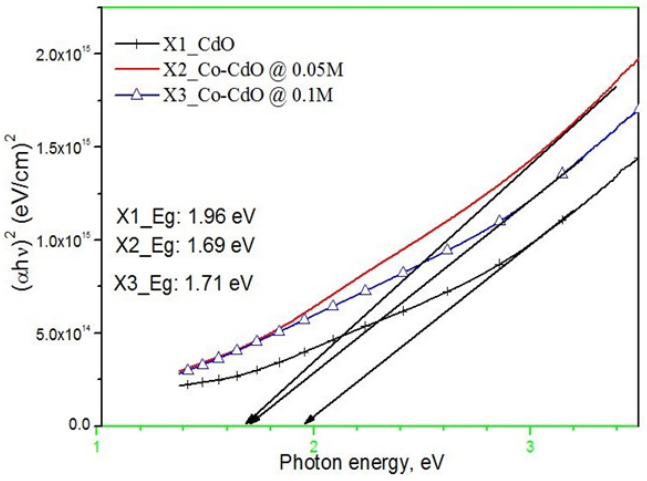

Figure 5: Tauc's plot for the CdO and Co-CdO thin films

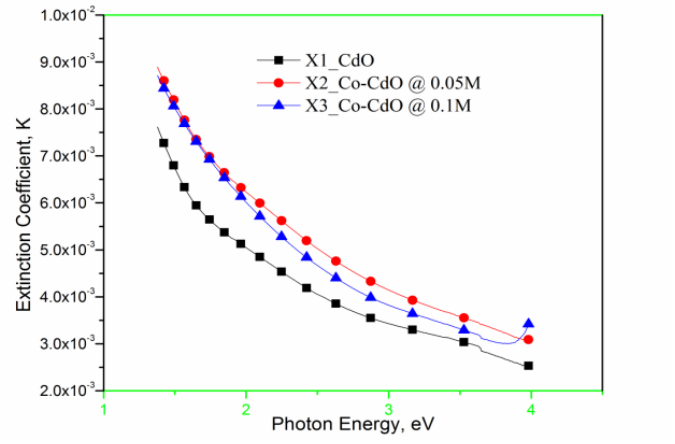

Figure 6: Extinction coefficient, k upon the photon energy

gap narrows as Co ion concentration rises. The structural and morphological changes, as well as the fact that Co ions have been known to introduce some energy levels in the CdO band gap close the valence band edge, are attributed for the reduction in the optical band gap of CdO after Co-doping [10].

3.4.3. Extinction coefficient

Extinction coefficient (k) is crucial in determining a variety of optical measurements, particularly those that are connected to the dielectric constants and light wave's absorption in a medium. The percentage of light lost due to scattering and absorption per unit of the penetrating medium is measured by the extinction coefficient, k value [3,21]. Extinction coefficient, k for all the samples was calculated from the relation [16]:

$$k = \frac{\propto \lambda}{4\pi}. \tag{9}$$

Fig. 6 shows the dependence of k upon the energy of the photon. It is depicted that k decreases as the incident photon energy increases and vice versa. This behaviour represents a strong absorption. It is seen from the figure that sample X1, the pure CdO has the lowest magnitude across the incident photon energy region of around2.5×10^{-3}.

3.4.4. Refractive index

Another significant optical constant is refractive index (n), which is critical in choosing the right materials to create optical devices or to use in optical applications. It provides details on the polarization, phase velocity, and local fields of light in the material. In the present study, the value of n was derived from the relationship shown below [16].

$$n = \frac{1}{T_s} + \left(\frac{1}{T_s - 1}\right)^{1/2}, \tag{10}$$

where T_s represents percentage transmission coefficient. Fig. 7 illustrates the dependence of refraction of the deposited samples upon the photon energy. For all samples, it can be seen that the refractive index keeps increasing at the higher energy with the least value of around 0.4 for the pure sample and 0.7 for the doped sample. It is important to notice that n values were practically unchanged at lower incident photon energies. The matching of the incident photon frequency and plasma frequency values could be the cause of the behaviour described above.

3.4.5. Optical conductivity

Optical band gap, refractive index, absorption coefficient, incident photon frequency, and extinction coefficient are the major parameters that determined the optical conductivity (σ_{opt}) of any material. In the present study, the value of optical conductivity was calculated from:

$$\sigma_{opt} = \frac{\alpha nc}{4\pi}, \tag{11}$$

where c and α are the speed of light and optical absorption coefficient, respectively. The behaviour of optical conductivity of the deposited films is shown in Fig. 8. It is seen that the samples have considerably high values of optical conduction with the least value around 1×10^{13} $(\Omega m)^{-1}$. The obtained results showed that the films exhibit excellent optical conductivity [16]. The optical conductivity of the material has been found to

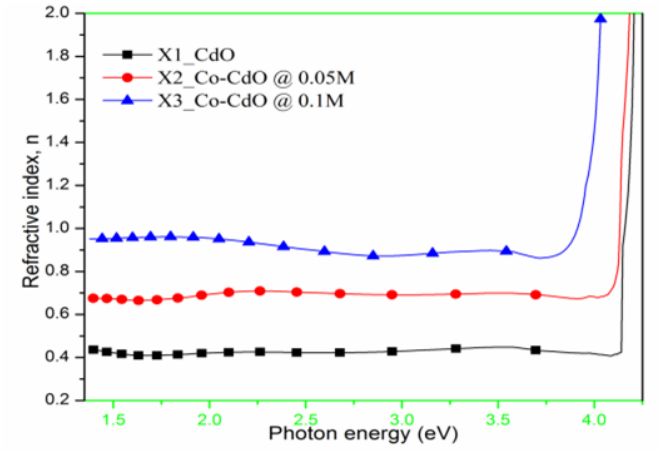

Figure 7: Variation of refractive index against the incident photon energy for the CdO and doped CdO

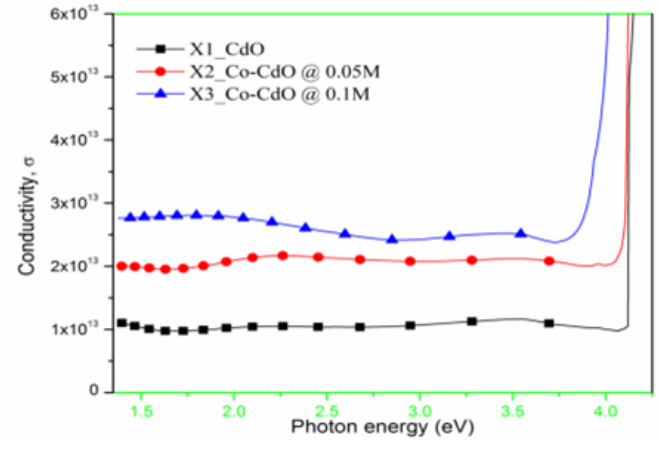

Figure 8: Optical conductivity of the films against the incident photon energy

increase with the increase in photon energy. The observed increase in the optical conductivity can be attributed to increase in density of localized states in the energy band [21]. Introduction of Co-dopant in the matrix of CdO have been seen to effectively enhance the conductivity of the material.

3.4.6. *High frequency dielectric constant*

High frequency dielectric constant is estimated in the present study by using [3].

$$n^2 = \varepsilon_\infty - \frac{1}{4\pi^2\varepsilon_o}\left(\frac{e^2}{c^2}\right)\left(\frac{N_{opt}}{m^*}\right)\lambda^2, \qquad (12)$$

where the parameters, e is the electronic charge, N_{opt} is the number of the carrier concentration, c denotes speed of light, ε_o is permittivity of free space and m* represents effective mass of the charge carriers. Plot of square of refractive index, n^2 against the square of wavelength, λ^2 yields a straight line. Extrapolating this line intercepts the n^2-*axis* (at $\lambda^2 = 0$). The obtained values after extrapolation correspond to high frequency dielectric constant, ε_∞. Fig. 9 revealed the representation of n^2 against λ^2. It is observed that the obtained values for all the samples are dependent on the dopant molar concentration.

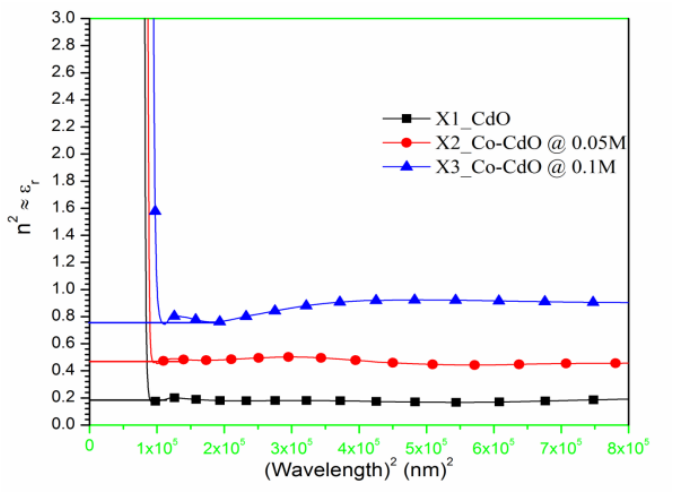

Figure 9: Representation of n^2 against λ^2 for the determination of ε_∞ of the deposited thin films

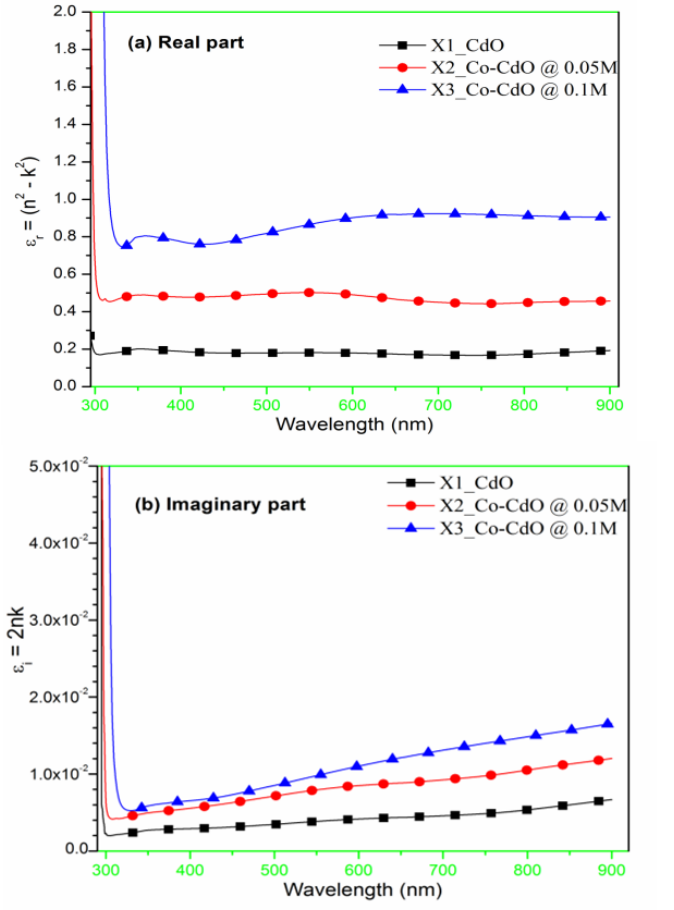

Figure 10: Variation of dielectric constants (a) Real part; (b) Imaginary part of the thin films

3.4.7. *Complex dielectric constant*

Another crucial characteristic of materials that have both real, ε_r and imaginary, ε_i parts is the complex dielectric con-

stant. This is related ε_r and ε_i parts according to the following

$$\varepsilon^* = \varepsilon_r + i\varepsilon_i, \tag{13}$$

where the real part of dielectric constant, ε_r gives information about the dispersion of light waves that propagates inside the material medium and it's also characterize for slowdown of this light as it travels through the materials while the energy absorption by an electric field resulting from dipole motion is represented by the imaginary part, ε_i. The ε_r and ε_i can be calculated using the following formulae [3,16]:

$$\varepsilon_r = n^2 - k^2, \tag{14a}$$

$$\varepsilon_i = 2nk. \tag{14b}$$

Fig. 10(a and b) illustrates the relationship between the deposited films' ε_r and ε_i values and the incident wavelength. The two graphs are seen to be relatively similar. It is also observed that ε_r of dielectric constant is greater than that of ε_i ($\varepsilon_r >> \varepsilon_i$). This can be attributed to ε_r strongly depend on the refractive index as n >>k. Likewise, the values of ε_i depends on the values of k. therefore the small value of k reduces the values of product, nk. The figures also revealed that the sequentially rising in the real and imaginary parts of the dielectric constant can be associated with increase in the dopant molar concentration.

4. Conclusion

An home-grown, cost-effective and environmental friendly two-electrode electrodeposition technique has been successfully used to grow polycrystalline thin film of CdO and Co-CdO on indium tin oxide coated glass substrates at ambient temperature. Results from EDX analysis revealed all the expected elements. Microstructural SEM images as corroborated by the XRD analysis revealed that the deposited samples are of polycrystalline cubic structure of CdO thin films. The average particle size of the films increases as the molar concentration of the Co-dopant increases. Optical and all the studied dielectric parameters showed that the samples' properties are greatly dependent on Co ion concentration. The optical band gap tuning was observed with variation in molar concentration of the dopant in the lattice of CdO. The study has successfully revealed a novel solution growth route of tuning the physical properties of CdO thin films by incorporation of Co ion dopant.

Acknowledgment

The authors gratefully appreciate the efforts of members of staff at the Physics Department, University of Pretoria, South Africa for the assistance on XRD and SEM characterization.

References

[1] R. L. Mishra, A. K. Sharma & S. G. Prakash, "Gas sensitivity and characterization of cadmium oxide (CdO) semi conducting thin film deposited by spray pyrolysis technique", Digest Journal of Nanomaterials and Biostrutures **4** (2009) 511.

[2] S. A. Adewinbi, W. Buremoh, V. A. Owoeye, Y. A. Ajayeoba, A. O. Salau, H. K. Busari, M. A. Tijani & B. A. Taleatu, "Preparation and characterization of TiO_2 thin film electrode for optoelectronic and energy storage Potentials: Effects of Co incorporation", Chemical Physics Letters **779** (2021) 138854. https://doi.org/10.1016/j.cplett.2021.138854

[3] A. S. Hassanien, "Studies on dielectric properties, opto-electrical parameters and electronic polarizability of thermally evaporated amorphous $Cd_{50}S_{50-x}Se_x$ thin films", Journal of Alloys and Compounds **671** (2016) 566. https://doi.org/10.1016/j.jallcom.2016.02.126

[4] A. M. Bazargan, S. M. A. Fateminia, M. Esmaeilpour Ganji & M. A. Bahrevar, "Electrospinning preparation and characterization of cadmium oxide nanofibers", Chemical Engineering Journal **155** (2009) 523. https://doi.org/10.1016/j.cej.2009.08.004

[5] E. T. Salim, R. A. Ismail, M. A. Fakhri, B. G. Rasheed & Z. T. Salim, "Synthesis of cadmium oxide/Si heterostructure for two-band sensor application", Iranian Journal of Science and Technology, Transactions A: Science **43** (2019) 1337. https://doi.org/10.1007/s40995-018-0607-8

[6] Z. Guo, M. Li & J. Liu, "Highly porous CdO nanowires: preparation based on hydroxy-and carbonate-containing cadmium compound precursor nanowires, gas sensing and optical properties", Nanotechnology **19** (2008) 245611. https://doi.org/10.1088/0957-4484/19/24/245611

[7] H. B. Lu, L. Liao, H. Li, Y. Tian, D. F. Wang, J. C. Li, Q. Fu, B. P. Zhu and Y. Wu. "Fabrication of CdO nanotubes via simple thermal evaporation", Materials Letters **62** (2008) 3928. https://doi.org/10.1016/j.matlet.2008.05.010

[8] R. A. Busari, B. A. Taleatu, S. A. Adewinbi, O. E. Adewumi, E. Omotoso, K. O. Oyedotun & A. Y. Fasasi, "Synthesis and surface characterization of electrodeposited quaternary chalcogenide $Cu_2Zn_xSn_yS_{1+x+2y}$ thin film as transparent contact electrode", Bulletin of Material Science **43** (2020) 1. https://doi.org/10.1007/s12034-019-2030-y

[9] S. A. Adewinbi, B. A. Taleatu, R. A. Busari, V. M. Maphiri, K. O. Oyedotun & N. Manyala, "Synthesis and electrochemical characterization of pseudocapacitive α-MoO_3 thin film as transparent electrode material in optoelectronic and energy storage devices", Materials Chemistry and Physics **264** (2021) 124468. https://doi.org/10.1016/j.matchemphys.2021.124468

[10] B. Sahin, F. Bayansal, M. Yüksel & H. A. Çetinkara, "Influence of annealing to the properties of un-doped and Co-doped CdO films", Materials Science in Semiconductor Processing **18** (2014) 135. https://doi.org/10.1016/j.mssp.2013.11.014

[11] A. A. Dakhel & M. Bououdina, "Development of transparent conducting copper and iron co-doped cadmium oxide films: Effect of annealing in hydrogen atmosphere", Materials science in semiconductor processing **26** (2014) 527. https://doi.org/10.1016/j.mssp.2014.05.015

[12] K. Gurumurugan, D. Mangalaraj & Sa. K. Narayandass, "Structural characterization of cadmium oxide thin films deposited by spray pyrolysis", Journal of crystal growth **147** (3-4) (1995) 355. https://doi.org/10.1016/0022-0248(94)00634-2

[13] R. Aydin & B. Şahin, "Comprehensive research on physical properties of Zn and M (M: Li, Na, K) double doped cadmium oxide (CdO) nanostructures using SILAR method", Ceramics International **43** (2017) 9285. https://doi.org/10.1016/j.ceramint.2017.04.087

[14] S. A. Adewinbi, R. A. Busari, L. O. Animasahun, E. Omotoso & B. A. Taleatu, "Effective pseudocapacitive performance of binder free transparent α-V_2O_5 thin film electrode: Electrochemical and some surface probing", Physica B: Condensed Matter **621** (2021) 413260. https://doi.org/10.1016/j.physb.2021.413260

[15] H. A. Mohamed, "p-Type transparent conducting copper-strontium oxide thin films for optoelectronic devices", The European Physical Journal-Applied Physics **56** (2011). https://doi.org/10.1051/epjap/2011100463

[16] S. Yasmeen, F. Iqbal, T. Munawar, M. A. Nawaz, M. Asghar & A. Hussain, "Synthesis, structural and optical analysis of surfactant assisted ZnO–NiO nanocomposites prepared by homogeneous precipitation method", Ceramics International **45** (2019) 17859.https://doi.org/10.1016/j.ceramint.2019.06.001

[17] L. O. Animasahun, B. A. Taleatu, S. A. Adewinbi, H. S. Bolarinwa & A. Y. Fasasi, "Synthesis of SnO_2/CuO/SnO_2 Multi-layered Struture for Photoabsorption: Compositional and Some Interfacial Structural Studies", Journal of Nigerian Society of Physical Sciences **3** (2021) 74. https://doi.org/10.46481/jnsps.2021.160

[18] D. S. Dhawale, D. P. Dubal, M. R. Phadatare, J. S. Patil & C. D.

Lokhande, "Synthesis and Characterizations of CdS nanorods by SILAR method: effect of film thickness", Journal of Materials Science **46** (2011) 5009. https://doi.org/10.1007/s10853-011-5421-z

[19] R. A. Busari, B. A. Taleatu, S. A. Adewinbi, O. E. Adewumi & A. Y. Fasasi, "Surface Characterisation of Spin Coated Quaternary Chalcogenide CZT (S, O) Thin Film for Optoelectronic Applications", Journal of Photonic Materials and Technology **5** (2019) 38. https://doi.org/10.11648/j.jmpt.20190502.13

[20] M. K. R. Khan, M. A. Rahman, M. Shahjahan, M. M. Rahman, M. A. Hakim, D. K. Saha & J. U. Khan, "Effect of Al-doping on optical and electrical properties of spray pyrolytic nanocrystalline CdO thin films", Current Applied Physics **10** (3) (2010) 790. https://doi.org/10.1016/j.cap.2009.09.016

[21] I. L. Ikhioya, E. Danladi, O. D. Nnanyere & A. O. Salawu, "Influence of Precursor Temperature on Bi Doped ZnSe Material via Electrochemical Deposition Technique for Photovoltaic Application", Journal of the Nigerian Society of Physical Sciences **4** (2022) 123. https://doi.org/10.46481/jnsps.2022.502